Intermetallic Phases in the Magnesium–Palladium System: X-ray Absorption Spectroscopic Characterization of the Amorphous Alloy $MgPdC_xH_y$

Deborah J. Jones and Jacques Rozière*

Laboratoire des Agrégats Moléculaires et Matériaux Inorganiques, URA CNRS 79, Université Montpellier 2, 34095 Montpellier Cedex 5, France

Lorraine E. Aleandri,* Borisav Bogdanović, and Sara C. Huckett†

Max Planck Institut für Kohlenforschung, Kaiser Wilhelm Platz 1, 4330 Mülheim an der Ruhr, Germany

Received November 12, 1991. Revised Manuscript Received January 31, 1992

Novel magnesium intermetallics produced via organometallic chemistry may be potential hydrogen storage systems. Nonmetallic components, i.e., interstitial carbon and hydrogen, are surmised to participate in defining both the local and the longer range order. In the magnesium–palladium system, $MgPdC_xH_y$ (x = 0.4–0.6; y = 0.8–1.9), prepared in tetrahydrofuran at <25 °C, remains X-ray amorphous, even after annealing. An X-ray absorption spectroscopic study of this compound, by reference to the crystalline magnesium palladium bimetallics MgPd and $Mg_{0.9}Pd_{1.1}$, as well as to $PdC_{0.15}$ and metallic palladium, has allowed its local environment to be identified as closely resembling that of $Mg_{0.9}Pd_{1.1}$ (HgMn arrangement), where the body-centered site of the tetragonal unit cell (defined by palladium atoms) is partially occupied by magnesium (ca. 90%) and partially by palladium (ca. 10%). The interstitial carbon in $MgPdC_xH_y$ has been found to occupy the *ac* face-center positions. The proximity of carbon to magnesium atoms and the retention of carbon and hydrogen on annealing may be key factors in the failure of this system to crystallize, even after prolonged annealing at 650 °C. A Fourier transform difference analytical method applied to $PdC_{0.15}$ and Pd foil has provided evidence for Pd–C contributions to the overall EXAFS in the former, at distances entirely compatible with the occupation by carbon of octahedral sites within the cubic cell.

Introduction

Alloys in amorphous form ("metallic glasses") represent a research field of current interest. Technical applications may lie in the fields of electric transformers, magnetism, and aerospace where high mechanical strength and resistance to corrosion are needed.[1] Amorphous alloys are also being intensively studied as catalysts and superconductors.[2] Most amorphous or noncrystalline metals and intermetallics are prepared through rapid quenching from melts or deposition of metallic vapours.[3–5] However, it has recently been reported[6–9] that through reactions between catalytically prepared magnesium hydride (MgH_2*)[10] or organomagnesium compounds and various metal species in organic solvents under mild conditions (<25 °C), X-ray amorphous binary magnesium intermetallics containing hydrogen can be prepared. Their propensity to include hydrogen suggests that the synthetic route could be exploited to produce metal hydrides appropriate for hydrogen storage. Indeed, the reaction between MgH_2* and bis(η^3-allyl)nickel yields an amorphous magnesium nickel hydride Mg_2NiH_2, which can subsequently undergo reversible dehydrogenation.[9]

In the magnesium–palladium system, the analogous reaction of bis(η^3-allyl)palladium with MgH_2* in a 1:2 ratio yields an amorphous hydride $Mg_2PdC_xH_2$ which, after dehydrogenation at 400 °C, can reabsorb hydrogen at 200–210 °C under high (10–90 bar) pressure of hydrogen.[7,8] Furthermore, dehydrogenation of the amorphous material leads to a novel crystalline compound $Mg_2PdC_{0.2-0.3}$.[11] Its Ti_2Ni-type structure, different from that of all other known phases in the magnesium–palladium system, is surmised to be stabilized by the presence of carbon on interstitial sites. In contrast, the reaction of bis(η^3-allyl)palladium with diethylmagnesium (1:2) gives a pyrophoric material $MgPdC_xH_y$, x = 0.4–0.6, y = 0.8–1.9, which remains amorphous even after annealing at 650 °C. ^1H and ^{13}C NMR have demonstrated that the formation of this material proceeds through an organobimetallic intermediate which undergoes elimination of the organic ligands.[6]

To define the local structural arrangement about palladium in $MgPdC_xH_y$, an X-ray absorption study has been undertaken of this amorphous material as isolated from the reaction solution and of other members of the magnesium–palladium system MgPd and $Mg_{0.9}Pd_{1.1}$. The EXAFS of metallic palladium and of palladium carbide $PdC_{0.15}$ are also reported.

Experimental Section

Materials. $MgPdC_xH_y$ (x = 0.4–0.6; y = 0.8–1.9) was synthesized as reported previously.[6,7] $Mg_{0.9}Pd_{1.1}$ and MgPd were obtained by high-temperature methods from the elements;[12] their powder X-ray diffraction patterns indicated the absence of any impurity. Pd foil (25 μm) was purchased from Alfa Products and was of >99.9% purity and $PdC_{0.15}$ was kindly provided by Dr. S. Ziemecki (Du Pont Experimental Station, Wilmington, DE). Mg_2PdC_x could not be utilized as a reference compound since the crystalline product[11] is unfailingly contaminated by small amounts of MgPd and $Mg_{2.7}Pd$.

† Present address: Los Alamos National Laboratories, INC-4 MS-C345, Los Alamos, NM.

(1) Warlimont, H. *Angew. Chem., Adv. Mater.* **1989**, *101*, 971.
(2) Steeb, S., Warlimont, H. Eds. *Rapidly Quenched Metals*; Proc. 5th Int. Conf., 1984, Würzburg, Germany; Vols. I and II. Armbruster, E.; Baiker, A.; Baris, H.; Güntherodt, H.-J.; Schlögl, R.; Walz, B. *J. Chem. Soc., Chem. Commun.* **1986**, 299.
(3) Duwez, P. *Prog. Solid State Chem.* **1966**, *3*, 377.
(4) Buckel, W.; Hilsch, R. *Z. Phys.* **1954**, *138*, 109.
(5) Schwartz, R. B.; Johnson, W. L. *Phys. Rev. Lett.* **1983**, *51*, 415.
(6) Bogdanović, B.; Huckett, S. C.; Wilczok, U.; Rufińska, A. *Angew. Chem.* **1988**, *100*, 1569.
(7) Bogdanović, B.; Huckett, S. C.; Spliethoff, B.; Wilczok, U. *Z. Phys. Chem. (Munich)* **1989**, *162*, 191.
(8) Bogdanović, B.; Huckett, S. C.; Spliethoff, B.; Wilczok, U. *Z. Phys. Chem. (Munich)* **1989**, *163*, 337.
(9) Bogdanović, B.; Claus; K.-H.; Gürtzgen, S.; Spliethoff, B.; Wilczok, U. *J. Less-Common Met.* **1987**, *131*, 163.
(10) Bogdanović, B. *Angew. Chem.* **1985**, *97*, 253.
(11) Norêus, D.; Bogdanović, B.; Wilczok. U. *J. Less-Common Met.* **1991**, *169*, 369.
(12) Kripyakevich, P. I.; Gladyshevskii, E. I. *Sov. Phys. Crystallogr.* **1960**, *5*, 552.

0897-4756/92/2804-0620$03.00/0

Spectroscopy. X-ray absorption spectra were recorded at the palladium K-edge at 77 K on the EXAFS 1 spectrometer at the French synchrotron facility, DCI at LURE, on two occasions having an interval of ca. 1 year, under typical beam conditions of 1.85 GeV, 200 mA. An identical experimental procedure was adopted on each occasion: the X-ray beam was monochromatized with a channel-cut Si(331) monochromator, and calibration of the spectrometer was performed before scanning using a 25-μm palladium foil by assigning the first maximum in the absorption edge as 24350 eV. Measurements were performed at 77 K in transmission mode in three energy regions using a step size of 2 eV over the edge region (24 330–24 400 eV), and 3 eV before and after this zone. Argon-filled ionization chambers were used to measure the incident and transmitted X-ray flux. No particular measures were taken to eliminate harmonics.

The intermetallic model compounds MgPd, $Mg_{0.9}Pd_{1.1}$, the interstitial phase $PdC_{0.15}$, and the unknown amorphous material $MgPdC_xH_y$ are all black powders. In each case, sampling was carried out immediately prior to recording of the EXAFS spectrum, under argon atmosphere to prevent any deterioration, by grinding and mulling the powders with paraffin oil stored over molecular sieves. Materials were then loaded and pressed between the parafilm windows of stainless steel sample holders so as to form homogeneous thin films free from pinholes or cracks. In each case at least three spectra were recorded of samples giving an increase in absorption over the edge of ca. 1.2. Different preparations of $MgPdC_xH_y$ (x = 0.45, y = 0.83 and x = 0.54, y = 1.29) were used in the two series of EXAFS experiments. All spectra were free from contamination by "glitches".

Data Analysis. All data analysis was performed using the programs developed by Michalowicz.[13] The X-ray absorption spectra were subjected to background removal and normalization using standard techniques [linear preedge function, removal of background curvature using a high (5th–6th) order polynomial or by a spline polynomial with division of the absorption spectrum into zones selected manually] and were selected to give the best signal-to-noise ratio and minimum mean standard deviation. The resulting average spectra $\chi(k)$ vs k are represented in Figure 1. Fourier transformation was carried out over a range typically 2.5–16 Å^{-1} using a Hamming window and k^3 weighting (Figure 2). Quantitative analysis using curve-fitting procedures was performed on Fourier-filtered spectra, back-transformed to reciprocal space, by systematically varying the coordination number N_i (this was however fixed at crystallographic values for the reference compounds), the Debye–Waller factor σ_i, and R_i, the distance of the ith shell of atoms from the absorber. For all of the compounds, the peaks in the Fourier transform (FT) are composite (containing contributions from more than one atom shell) and calculations were first carried out on one-peak filtered spectra to minimize the number of parameters varied and correlation between terms, before attempting a two-peak fit (range in R space 1.5–5 or 6 Å), containing up to five atom shells.

For the model compounds MgPd, $Mg_{0.9}Pd_{1.1}$, and $PdC_{0.15}$, the phase and amplitude functions used were the ab initio calculated values of McKale.[14] These gave satisfactory agreement with known structures when allowance was made for changes in the energy origin E_o and for variations in the photoelectron mean free path, for each type of atom shell. These values were then adopted in calculations on $MgPdC_xH_y$.

Fourier Difference Analysis. The FT of $PdC_{0.15}$ and Pd foil were filtered over identical R-space limits, 1.6–3.2 Å. Slight adjustment in k space accounted for the small increase in Pd–Pd distance caused by inclusion of carbon in the metal lattice. The difference EXAFS spectrum $[\chi(k)_{expt,PdC_{0.15}} - \chi(k)_{calc,Pd}]$ was then Fourier transformed.

Structure of Model Compounds. Palladium metal has an *fcc* structure of unit cell length, a = 3.890 Å.[15] Each palladium atom has 12 nearest neighbors at a distance of $a/\sqrt{2}$ and 6 next-nearest neighbors at the corners of the unit cell. In $PdC_{0.15}$, where the unit cell is slightly expanded to 3.996 Å,[16] the carbon atoms have recently been reported to occupy octahedral sites at the cube-center and edges. Of the intermetallic phases, MgPd has a CsCl type cubic lattice, a = 3.17 Å,[12] while $Mg_{0.9}Pd_{1.1}$ adopts the tetragonal HgMn type arrangement, with a = 3.03 Å, c = 3.42

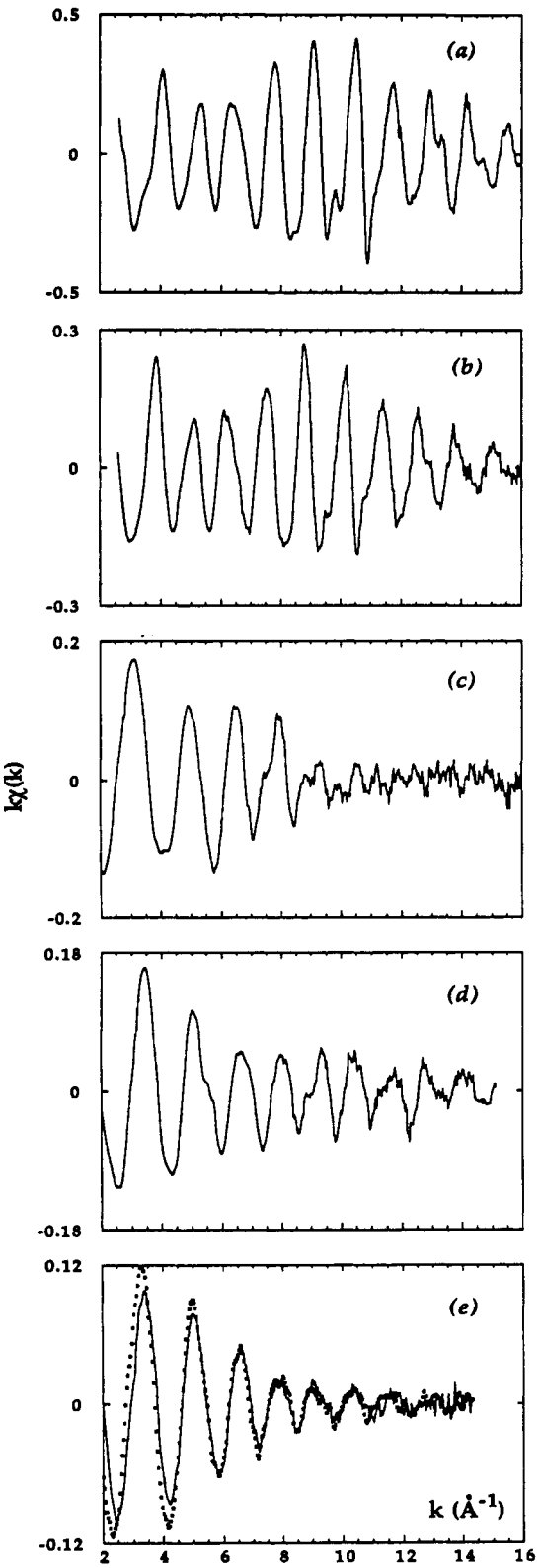

Figure 1. Background subtracted and normalized EXAFS data for (a) Pd foil, (b) $PdC_{0.15}$, (c) MgPd, (d) $Mg_{0.9}Pd_{1.1}$, (e) $MgPdC_xH_y$. Data from two experimental runs of different preparations are shown.

(13) Michalowicz, A. In *Structures Fines d'Absorption X en Chimie Vol. 3 Logiciels d'Analyse*: EXAFS pour le Mac.; Dexpert, H., Michalowicz, A., Verdaguer, M., Eds.; CNRS Press, 1988.
(14) McKale, A. G. *J. Am. Chem. Soc.* **1988**, *110*, 3703.
(15) Nayeb-Hashemi, A. A.; Clark, J. B. *Bull. Alloy Phase Diagrams* **1985**, *6*, 164.
(16) Ziemecki, S. B.; Jones, G. A.; Swartzfager, D. G.; Harlow, R. L. *J. Am. Chem. Soc.* **1985**, *107*, 4547.

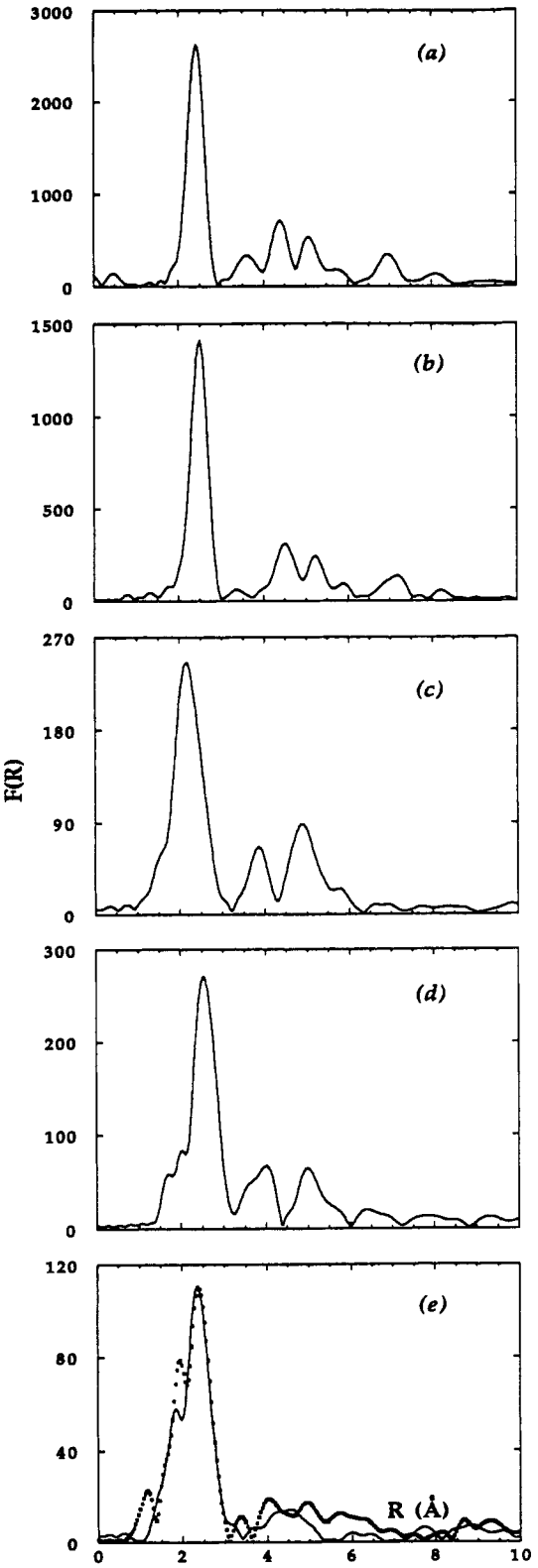

Figure 2. Fourier transformed EXAFS spectra of (a) Pd foil, (b) $PdC_{0.15}$, (c) MgPd, (d) $Mg_{0.9}Pd_{1.1}$, (e) $MgPdC_xH_y$. Data from two experimental runs of different preparations are shown.

Å, in which 90% of the body-center sites are occupied by Mg and 10% by palladium.[12] This complexity excludes its use in the derivation of experimental phase and amplitude functions, but the compound served as a valuable model for $MgPdC_xH_y$.

Results and Discussion

I. Model Compounds. *Metallic Pd.* The FT (Figure 2a) is dominated by an intense peak, the maximum of which, after phase correction, occurs at ca. 2.7 Å. At longer distances, three further maxima between 3 and 6 Å correspond to Pd–Pd contributions at distances a, $a\sqrt{3}/2$, and $a\sqrt{2}$ (face diagonal). Equivalent EXAFS spectra are given by metallic rhodium or platinum.[17] The results of nonlinear least-squares fitting on these four shells (Table I) were consistent with the crystallographic result. However, it is noted that the linearity of palladium atoms in this system (and, indeed, in others considered here) is such that multiple scattering contributions to the EXAFS are probably not negligible, and changes in amplitude and phase of the photoelectron may occur when passing through the atom—the "lens" atom—lying between the absorber and backscatterer.

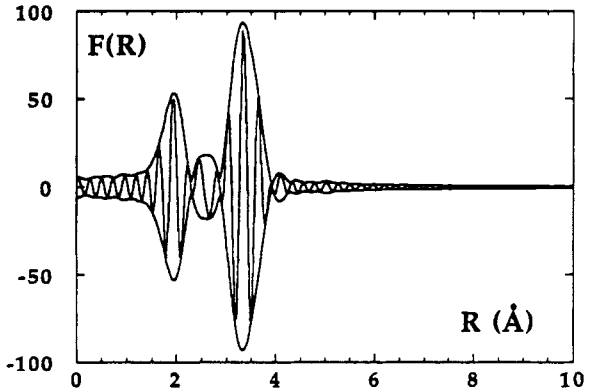

Figure 3. Difference Fourier transform of $[\chi(PdC_{0.15}) - \chi(Pd)]$ after phase correction for the Pd–C pair. See text for details.

$PdC_{0.15}$. As expected, the absorption spectrum and the FT spectrum of $PdC_{0.15}$ (Figure 2b) closely resemble those of metallic palladium, and the *fcc* lattice is clearly retained. In view of the minor contribution of carbon relative to that of palladium toward the overall EXAFS, in a first step only the metal–metal contribution was introduced into the curve-fitting routines. Using either theoretical or experimental phase and amplitude parameters (extracted from the first peak in the FT of palladium metal) gave agreement to within 5% for coordination number and, for the bond length, ±0.005 Å of the crystallographic value. To isolate the two carbon components of this peak, a second approach was used, namely, a "difference" EXAFS technique. The structural similarity of $PdC_{0.15}$ and metallic palladium allows cancellation of the spectral signature common to both compounds (after slight adjustment to allow for lattice expansion in $PdC_{0.15}$) and the consequent manifestation of contributions arising from the Pd–C pair. The two major peaks in the difference FT spectrum (Figure 3) at 1.96 and 3.46 Å, after correction for the Pd–C phase shift, correspond to carbon atoms in octahedral sites in the parent platinum structure. These bond lengths are compatible with the values expected from neutron powder diffraction, $a/2$ and $\sqrt{3}a/2$.[16] Furthermore, the result is in agreement with position of boron, as determined by EXAFS, in the closely related $PdB_{0.16}$.[18] A minor contribution to the difference FT, centered at ca. 2.8 Å, corresponds to a residue of the Pd–Pd contribution remaining after subtraction.

The Pd–C bond lengths were subsequently introduced into a curve fit to the total experimental EXAFS over the first peak, and including Pd–Pd and two Pd–C shells. Given the stoichiometry $PdC_{0.15}$, 0.9 and 1.2 nearest carbon neighbors are expected for the shells at 1.96 and 3.46 Å, respectively, close to the values obtained after least-squares

(17) Via, G. H.; Sinfelt, J. H.; Lytle, F. W. *J. Chem. Phys.* **1979**, *71*, 690.
(18) Lengeler, B. *Solid State Commun.* **1985**, *55*, 679.

Table I. Comparison of Structural Parameters Derived from EXAFS Spectroscopy for Pd Foil, $PdC_{0.15}$, MgPd, $Mg_{0.9}Pd_{1.1}$, and $MgPdC_{0.45}H_{0.83}$ and Calculated from Diffraction Data for Pd Foil, $PdC_{0.15}$, MgPd, and $Mg_{0.9}Pd_{1.1}$[a]

	shell	N	σ, Å	γ	R_{exp}, Å	R_{th}, Å	ΔE, eV	Res, %	geom relation
Pd	Pd	12	0.08 (2)	1.1 (1)	2.74 (4)	2.75	−19		$a/\sqrt{2}$
	Pd	6	0.10 (4)	1.3 (5)	3.87 (3)	3.89	−20		a
	Pd	24	0.09 (1)	1.6 (3)	4.76 (4)	4.76	−21		$a\sqrt{(3/2)}$
	Pd	12	0.07 (1)	1.8 (3)	5.44 (9)	5.50	−12	2.4	$a\sqrt{2}$
$PdC_{0.15}$	C	0.8 (2)	0.05 (2)	1.1 (3)	1.95 (1)	1.99	−11		$a/2$
	Pd	12	0.06 (2)	1.1	2.81 (1)	2.83	−16		$a/\sqrt{2}$
	C	1.9 (10)	0.04 (4)	1.0 (1)	3.46 (4)	3.46	8	3.6	$(\sqrt{3}a)/2$
	Pd	6				3.99			a
	Pd	24	0.07 (1)	1.4 (4)	4.88 (1)	4.89	−20		$a\sqrt{(3/2)}$
	Pd	12	0.04 (1)	1.5 (2)	5.56 (3)	5.65	−12	9.0	$a\sqrt{2}$
MgPd	Mg	8 (1)	0.08 (1)	1.0 (3)	2.78 (2)	2.75	−12		$\sqrt{(3a^2)}/2$
	Pd	6 (2)	0.11 (2)	2.1 (4)	3.13 (7)	3.17	−20	3.1	a
$Mg_{0.9}Pd_{1.1}$	Mg	7.2	0.09 (1)	1.1 (2)	2.74 (5)	2.74	−9		$(2a^2 + c^2)^{1/2}/2$
	Pd	0.8	0.04 (1)	2.1 (3)	2.76 (2)	2.74	−17		
	Pd	4	0.06 (1)	2.1 (2)	3.03 (2)	3.02	−17	1.4	a
	Pd	2				3.41			c
	Pd	4	0.07 (2)	1.8 (3)	4.26 (7)	4.27	−20		$a\sqrt{2}$
	Pd	8	0.09 (2)	2.2 (4)	4.53 (3)	4.55	−20		$(a^2 + c^2)^{1/2}$
$MgPdC_xH_y$	C	0.5 (4)	0.02 (3)	1.1	2.35 (7)		−11		
	Mg	6.1 (5)	0.10 (1)	1.1	3.78 (8)		−9		
	Pd	0.8 (6)	0.07 (3)	2.0	2.78 (5)		−17		
	Pd	4.1 (7)	0.13 (3)	2.0	3.08 (6)		−17	1.2	

[a] N: number of atoms in the shell; σ: Debye–Waller factor; R; distance from the Pd absorber, ΔE: shift in the energy origin; γ: photoelectron mean free path. [b] $\text{Res} = \sum_k(k[\chi_{exp}(k)] - k[\chi_{th}(k)])^2k^3/\sum_k(k[\chi_{exp}(k)]^2)k^3$.

refinement (Table I). Although the X-ray absorption technique is unable to provide such information, random occupation of the octahedral sites is expected. For longer Pd–Pd distances, in the region of the second main peak in the FT spectrum, the 24- and 12-atom shells at 4.89 and 5.65 Å, respectively, converged rapidly, but inclusion of the 6-atom shell at 3.99 Å caused no further improvement to the fit.

MgPd. Fourier transformation over the range 2.5–12 $Å^{-1}$ gave the radial distribution function displayed in Figure 2c. Of the three main peaks, the first is expected, from calculation using the unit cell parameter 3.16 Å, and symmetry of the *Pm3m* space group, to result from 8 magnesium and 6 palladium atoms at 2.74 and 3.17 Å, respectively (body center and corner sites), the second from 12 Pd on face-center diagonal sites with respect to the origin, (Pd–Pd = 4.48 Å), and the third from longer distance magnesium (12 at 5.26 Å) as well as body center diagonal palladium atom (8 at 5.49 Å) contributions. Fourier filtering over the first peak and back-transformation into k-space, allowed the EXAFS of the first two coordination shells to be tested against the crystallographic result,[12] by systematically and successively adjusting values of the Pd–Pd and Pd–Mg distances, the E_0 offset, the electron mean free path, and the Debye–Waller factor, while respecting the number of independent parameters to be varied, $N_{ind} - 1$, where $N_{ind} = 2\Delta R\Delta k/\pi$. The results of these refinements is given in Table I.

$Mg_{0.9}Pd_{1.1}$. The FT of this phase displays three principal peaks (Figure 2d). From calculations using the lattice parameters determined by X-ray powder diffraction, the first of these peaks is expected to contain four components, being palladium atoms at distances corresponding to a and c (3.03 and 3.42 Å respectively), and the body-center atoms at 2.73 Å, composed of 90% Mg and 10% Pd over all crystal space. At greater distance, the second and third peaks are also composite and contain two palladium shells (4.27, 4.55 Å) and palladium and magnesium contributions (5.07–5.54 Å), respectively. For the first of these peaks, successive introduction of Pd and Mg phase corrections (after adjustment of E_0) into the calculation of the FT spectrum agreed with these data, and subsequent curve fitting to the EXAFS equation[19] indicated that the spectrum could adequately account for the disordered body-center site (Table I). However, the contribution to the EXAFS of the palladium atom shell at distance c was found to be insignificant and, although there is no one clear reason for this effect (anisotropic Debye–Waller factor, destructive interference induced by multiple scattering effects etc.), this shell was discarded in a final calculation without detriment to the overall satisfactory agreement.

II. Structural Characterization. *$MgPdC_xH_y$.* Figure 1e illustrates the practical identity of the EXAFS derived from absorption spectra given by two different preparations of $MgPdC_xH_y$ recorded on two separate experimental runs at a one-year interval and, for clarity, we limit the following discussion to the result obtained on $MgPdC_{0.45}H_{0.83}$ sample. In a first qualitative appraisal, the absorption spectrum and derived EXAFS are similar to those of the nonstoichiometric intermetallic $Mg_{0.9}Pd_{1.1}$. On Fourier transformation, Figure 2e, only a single peak (of two maxima) is observed, with an additional structure at ca. 4.6 Å rising above the background.

Initial values of Pd–Mg and Pd–Pd bond lengths were obtained from the FT spectrum (2.75 and 3.08 Å, respectively). These distances are almost identical to those observed in $Mg_{0.9}Pd_{1.1}$. A first model based on a magnesium atom shell and a palladium shell at 3.08 Å gave good agreement with the experimental data, Figure 4a. The apparent structural similarity between this compound and $Mg_{0.9}Pd_{1.1}$ led to the testing of this model against the experimental EXAFS of $MgPdC_xH_y$ by the introduction of a second shell of Pd atoms at 2.78 Å (to account for the disordered body center site) and a longer distance palladium contribution at ca. 3.45 Å. The agreement between experimental and calculated curves at this stage was already satisfactory, but the inclusion of a carbon contribution at 2.35 Å further improved the overall result, which is reported numerically in Table I and graphically in Figure 4b.

The results for the two $MgPdC_xH_y$ samples are self-consistent and remarkably similar to those obtained on

(19) Stern, E. A. In *X-ray Absorption Fine Structure: Principles, Applications Techniques of EXAFS SEXAFS and XANES*; Koningsberger, D. C., Prins, R., Eds.; Wiley: New York, 1988; pp 1–51.

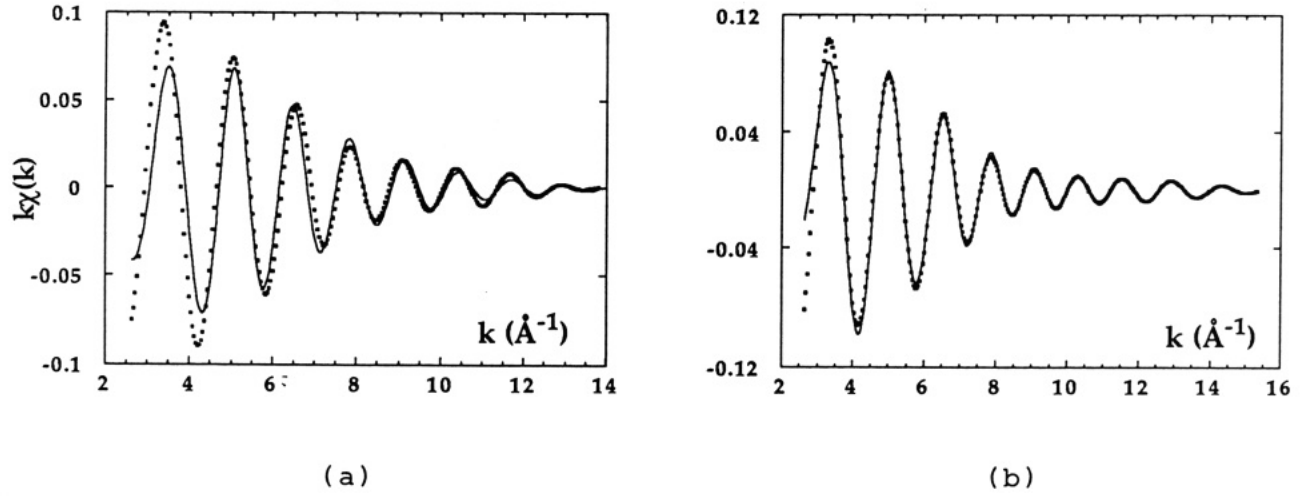

Figure 4. Fits to the backtransform of the first peak of the FT spectrum of $MgPdC_{0.45}H_{0.83}$. (a) Calculated spectrum includes only backscattering from Mg atoms, $R^* = 11\%$. (b) Calculated spectrum includes contributions from magnesium, palladium, and carbon atom shells, $R^* = 2\%$. * Quality of the fit as estimated from the residual factor R. ($R = \sum_k(k[\chi_{exp}(k)] - k[\chi_{th}(k)])^2k^3/\sum_k(k[X_{exp}(k)]^2)k^3$. ●, experimental; —, calculated.

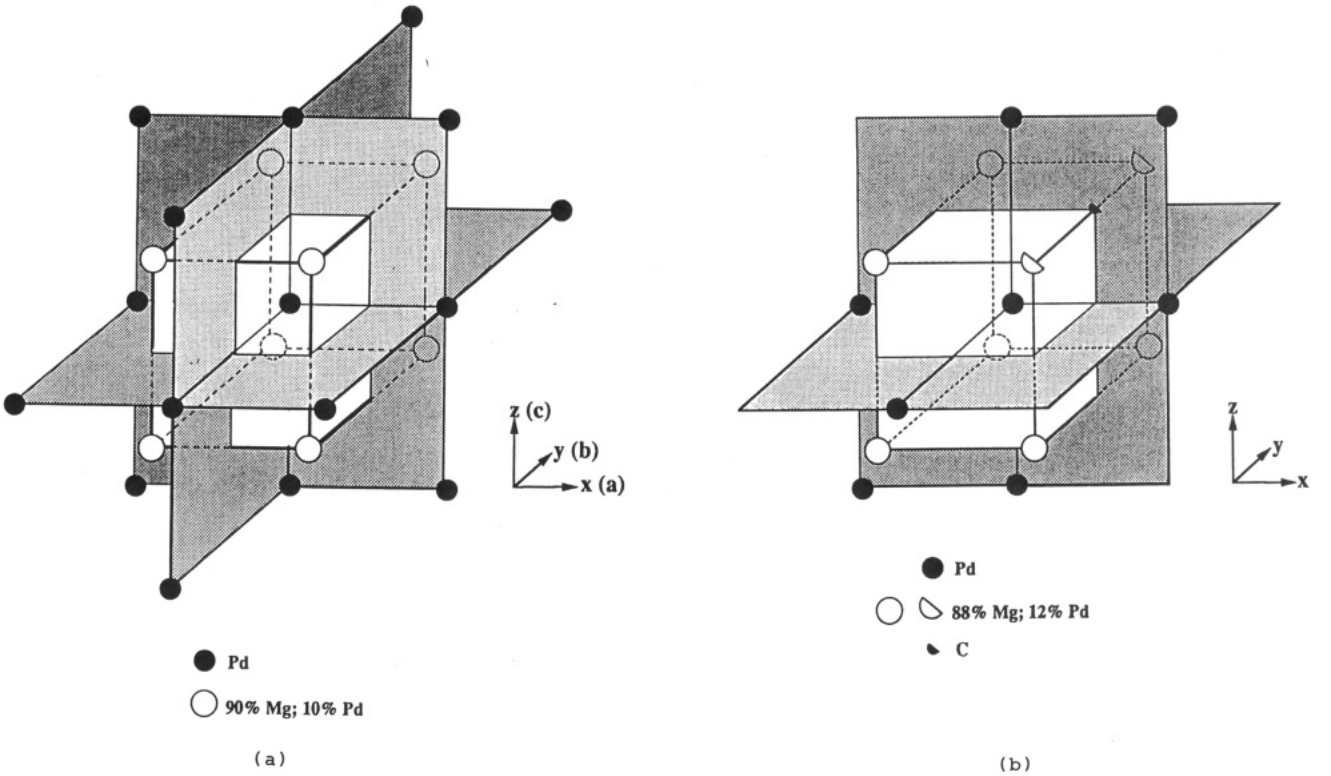

Figure 5. (a) Environment about palladium at (0,0,0) in a tetragonal unit cell of $Mg_{0.9}Pd_{1.1}$ (HgMn structure type). (b) Environment about palladium in $MgPdC_xH_y$.

$Mg_{0.9}Pd_{1.1}$. This similarity suggests that the short-range environment about palladium in $MgPdC_xH_y$ is related to that around palladium in $Mg_{0.9}Pd_{1.1}$.

In this latter compound, if attention is focused on the Pd atom at the 0,0,0 site and its eight surrounding unit cells, a distorted cubic coordination geometry about the metal atom can be defined, which consists of 7.2 magnesium atoms and 0.8 palladium atoms, giving the first Pd–Mg and Pd–Pd shells at 2.74 (5) and 2.76 (2) Å. The remaining Pd atoms out to 4.6 Å lie in three perpendicular planes, each of which bisects the Pd-atom-centered elongated cube $(Mg/Pd)_8$, Figure 5a: the *xy* plane containing Pd atoms along *a* and *b* (at 3.03 Å), and across the *ab* diagonal (4.26 Å); the *xz* and *yz* planes including Pd atoms along *c* at 3.41 Å and across the *ac* and *bc* diagonals, 4.53 (3) Å.

Employing this type of structural framework, local ordering about palladium in $MgPdC_xH_y$ can be envisaged (Figure 5b): the first Pd–Mg and Pd–Pd shells at 2.78 Å yield a primary mixed Mg/Pd distorted cubic coordination geometry about palladium metal. Additional Pd atoms are located on the *xy* plane from the central Pd atom at a distance of 3.08 (6), which is reminiscent of the Pd–Pd separation along *a* and *b* for $Mg_{0.9}Pd_{1.1}$. The observed Pd–C distance, 2.35 (7) Å, suggests that carbon is located at the center of the *ac* face. This is substantiated by the observation of Pd–Pd distances along the *ac* diagonal as indicated by the second peak in the FT centered at ca. 4.6 Å. The amplitude of this distant shell of palladium atoms may be increased through the lens effect[18] of the carbon atom, while the longer Pd–Pd *ab* diagonal type distances remain unobservable in the amorphous material. More

importantly, it may be surmised that the position of carbon within the MgPd framework actually prevents any long-range ordering on thermal treatment, since the simultaneous existence of carbon at the *ac* face center sites, and Mg/Pd at the body-center site in the unit cell is excluded, because of the proximity that this causes, 1.54 Å. In such a model, the number of body-center Mg/Pd atoms is expected to be reduced from the 8 expected, as observed experimentally (total Mg + Pd = 6.9 atoms).

Considering a central palladium atom surrounded by a total of 6.9 nearest neighbors, a final formula of $Mg_{0.9}Pd_{1.1}$ (Mg: 6.1/6.9; Pd: 1 + 0.8/6.9) can be derived from EXAFS, which is in good agreement with the 1:1 stoichiometry determined chemically. Furthermore, the reproducibility of the metal stoichiometry over a number of preparations employing an excess of magnesium [2 mol of $Mg(C_2H_5)_2$ to 1 mol of $Pd(\eta^3\text{-}C_3H_5)_2$] suggests that the amorphous intermetallic has a unique composition. The EXAFS results indicate that a distinct coordination sphere exists about palladium, as opposed to a random mix of amorphous metals and carbon. In addition, essentially the same environment is found in two preparations measured on two separate occasions. Both observations further demonstrate that the amorphous phase $MgPdC_xH_y$ exists as a defined intermetallic or, better, a carbide, with a uniform short-range structure.

With the exception of the carbon shell, the short-range ordering in $MgPdC_xH_y$ is a fragment of the crystal structure adopted by $Mg_{0.9}Pd_{1.1}$, i.e., HgMn. This conclusion is further supported by the recent observation that in the magnesium–platinum system, by using a synthetic route similar to that employed for the preparation of $MgPdC_xH_y$, a stoichiometric MgPt phase is formed, which is crystalline and which also adopts the HgMn arrangement.[20] It is important to stress that the only previously known MgPt compound, produced by high-temperature methods, crystallizes with an FeSi-type structure, which is markedly different from the HgMn type.

The amorphous intermetallic $MgPtC_{0.65}H_{2.98}$ obtained from the reaction of MgH_2' (a solubilized form of MgH_2[21]) with $PtCl_2$ in tetrahydrofuran at 25 °C can be converted easily to crystalline MgPt after thermal treatment for 24 h at 550 °C. However, in the case of $MgPdC_xH_y$, no transformation to a crystalline state can be achieved, even after annealing at 650 °C for 3 days. After annealing, the above MgPt compound contained only 0.06 C/Pt, whereas $MgPdC_xH_y$ (specifically, an $MgPdC_{0.6}H_{1.5}$ sample) retained a notably higher amount of carbon after similar treatment: 0.3 C/Pd, which further supports the supposition stated above that the presence of carbon and its location in the metal framework of $MgPdC_xH_y$ inhibits crystallization. This analytical result also suggests that carbon is not incorporated into the metal lattice of the amorphous $MgPtC_xH_y$ material, or at least not in the same manner as in its palladium analogue; verification of this hypothesis is currently underway by means of an X-ray absorption spectroscopic study of both amorphous and crystalline magnesium–platinum materials.

The role of carbon in the magnesium–palladium system seems significant to the eventual structure adopted by the metal lattice. For $MgPdC_xH_y$, the retention of carbon seems to prevent any transition to a crystalline phase, whereas the Ti_2Ni-type structure of crystalline $Mg_2PdC_{0.2}$ is believed to be stabilized by the incorporation of interstitial carbon. It has been shown recently that this Ti_2Ni type structure can also be stabilized by interstitial hydrogen in an isotypical magnesium–rhodium compound, $Mg_2RhH_{1.1}$,[22] and the influence of hydrogen in $MgPdC_xH_y$ cannot be underestimated. In the $MgPdC_{0.6}H_{1.5}$ sample fired at 650 °C for 3 days, the level of hydrogen content remained considerable at 0.6 H/Pd. Although not observed through the analysis of X-ray absorption spectra, hydrogen atoms could be accommodated in tetrahedral or octahedral sites in the magnesium–palladium framework.

Acknowledgment. We are indebted to Dr. S. B. Ziemecki (Du Pont Experimental Station, Wilmington, DE) for providing the sample of $PdC_{0.15}$, and we thank LURE for access to experimental stations.

Registry No. $MgPdC_{0.4\text{-}0.6}H_{0.8\text{-}1.9}$, 139244-62-5.

(20) Aleandri, L. E.; Wilczok, U.; Bogdanović, B., to be published.
(21) Bogdanović, B.; Bons, P.; Schwickardi, M.; Seevogel, K. *Chem. Ber.* **1991**, *124*, 1041.
(22) Bonhomme, F.; Yoshida, M.; Yvon, K.; Fischer, P. *J. Less-Common Met.*, in press.